Scientific Notebook 588E

Entry: John Stamatakos
Date: April 24, 2003

Title: **Evaluation of Faulting as it Relates to Postclosure Performance of the Proposed High-level Waste Repository at Yucca Mountain, Nevada.**

Personnel: John Stamatakos was the Principal Investigator of this project and was also the lead author of the report. The report was coauthored by David A. Ferrill, Deborah J. Waiting, Alan P. Morris, Darrell W. Sims, and Amitava Ghosh. All entries in this scientific notebook were made by John Stamatakos unless otherwise indicated in this text.

John Stamatakos developed the Executive Summary, Introduction (Chapter 1), and Conclusions (Chapter 5), provided the review and analyses of the DOE approach to faulting (Chapter 2), and developed the methodology used to evaluate the consequences and risk of faulting based on the FAULTO Module (Chapter 3). He also carried out all the risk computations (chapters 3 and 4).

David Ferrill, Darrell, Sims, and Alan Morris provided the summary information of analog earthquakes and the analog faulting methodology, which includes the derivations of fault trace-length densities and fault-drift intersection analysis (all in Chapter 4).

Deborah Waiting performed the TPA runs, reduced the TPA data, and developed the fault maps and maps of Yucca Mountain based on ArcView GIS© software.

Amitava Ghosh provided input on the probability distribution functions used to model faults in Chapter 3, as well as information on the application of the FAULTO Module to this problem.

Additional insights were gained by discussion with B. Hill, S. Mohanty, T. McCartin, A,B, Ibrahim, P. Justus, G. Wittmeyer, and O. Pensado. B. Hill provided the technical review. B. Long and K. Murphy did the editorial review. B. Sagar conducted the programmatic review. The administrative and format support was provided by R. Emmot. O. Pensado also provided some simple **MATHEMATICA Version 4.1** scripts to help manipulate the TPA data.

Project: This notebook document procedures, codes, data, and results used in support of conclusions reached in Intermediate Milestone **20.06002.01.061.330 — EVALUATION OF FAULTING AS IT RELATES TO POSTCLOSURE PERFORMANCE OF THE PROPOSED HIGH-LEVEL WASTE REPOSITORY AT YUCCA MOUNTAIN, NEVADA.** This text and supporting files are provided herein to meet the CNWRA requirements of QAP -001.

A preliminary paper on this topic, which described the two performance assessment methodologies we used for this report but not the data or results was presented at the 2003 International High-Level Radioactive Waste Management Conference. The paper was titled **Methodologies For The Evaluation of Faulting at Yucca Mountain, Nevada.** The authors were Deborah J. Waiting, John A. Stamatakos, David A. Ferrill, Darrell W. Sims, Alan P. Morris, Philip S. Justus, Abou-Bakr K. This paper was presented at the meeting by D. Waiting. The presentation files is included as a attachement to this electronic scientific notebook in the file: ***IHRWC_Faulting_presentation.ppt***. A .pdf version of the paper is also attached as ***IHLRWC_Faulting_paper.pdf.***

Scientific Notebook 588E

Entry: John Stamatakos
Date: April 24, 2003

Data: CNWRA data contained in this report meet quality assurance requirements described in the CNWRA Quality Assurance Manual. Data used to support conclusions in this report taken from documents published by the U.S. Department of Energy (DOE) contractors and supporting organizations were generated according to the quality assurance program developed by DOE for the Yucca Mountain Project.

Codes: Maps and related Geographic Information System (GIS) data were generated and plotted by the software ArcView GIS© Versions 3.1 (ESRI, 1998) and 3.2a (ESRI, 2000), which are commercially available software codes that are maintained in accordance with CNWRA Technical Operating Procedure TOP–018. Total system performance analyses were conducted using the Total-system Performance Assessment (TPA) Version 4.1j code[1] (Mohanty, et al., 2002), including the EBSREL, EBSFAIL, and NFENV modules, which are included in the TPA Version 4.1j code as well as the FAULTO module (Ghosh, et al., 1997). The TPA Version 4.1j code and FAULTO module were developed at the Center for Nuclear Waste Regulatory Analyses in accordance with CNWRA Technical Operating Procedure TOP–018. All other codes used in this report are standard versions of commonly used commercial codes including KaleidaGraph™ Version 3.09, Excell (97-SR2), and MATHEMATIC, Version 4.1.

References:

ESRI. "ArcView GIS©." Version 3.2a. Redlands, California: ESRI. 2000.

ESRI. "ArcView GIS©." Version 3.1. Redlands, California: ESRI. 1998.

Ghosh, A., R.D. Manteufel, and G.L. Stirewalt. "Faulting Version 1.0—A Code for Simulation of Direct Fault Disruption: Technical Description and User's Guide. San Antonio, Texas: CNWRA. 1997.

Mohanty, S., T.J. McCartin, and D.W. Esh. "Total-system Performance Assessment (TPA) Version 4.0 Code: Module Description and User's Guide." San Antonio, Texas: CNWRA. 2002.

---

[1] TPA Version 4.0 code is the last iteration of the user's guide. Version 4.1j, however, was used for calculations in this report. Despite several changes to the code in moving from Version 4.0 to 4.1j, the documentation in the user's guide for Version 4.0 remains applicable. Most revisions pertain to replacing old with new data as these were made available through the course of developing this report.

Scientific Notebook 588E

Entry: John Stamatakos
Date: April 24, 2003

Entry 1. Set up of the TPA inputs for Faulting

a) Model the Solitario Canyon and Ghost Dance faults in FAULTO Module
   (1) location/geometry - fixed based on mapping of Day, et al. (1998a, 1998b) - Figure 1
   (2) use old repository footprint with subareas (TPA version 4.1j) - Figure 2b.
   (3) sample fault width - lognormal PDFs based on ESF data (Mongano, et al., 1999) - Figure 3.

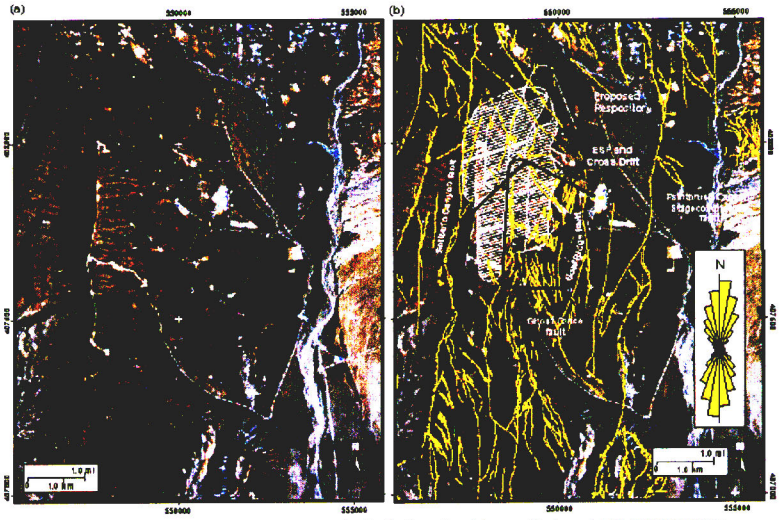

Figure 1 Natural color mosaic of IKONOS 2 satellite images showing the Yucca Mountain area. The images were captured between September 2000 and August 2002 and consist of panchromatic sharpened multispectral data. Figure (a) shows Yucca Mountain and the surrounding area. Figure (b) overlays faults (yellow lines) from Simonds et al. (1995), the Exploratory Studies facility (ESF), Cross Drift, and proposed repository layout from CRWMS M&O (2002). The inset rose diagram shows cumulative fault length in bins of 10-degree strike azimuths. Coordinates are in Universal Transverse Mercator (UTM) Zone 11, using the North American Datum of 1927.

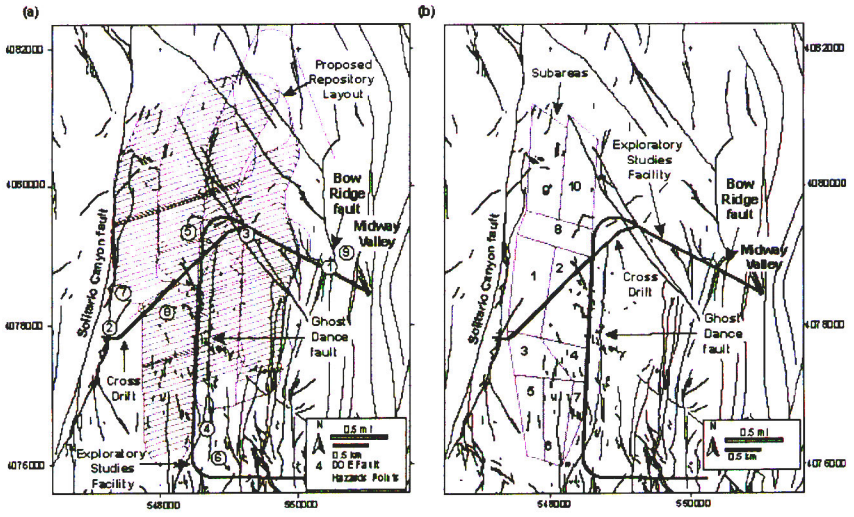

Figure 2. Maps showing proposed repository layouts relative to fault traces mapped at Yucca Mountain. Fault traces are from Day, et al. (1998a and 1998b). The more recently proposed repository layout (CRWMS M&O, 2002) is shown in (a) as are the locations of the nine demonstration points used in the DOE probabilistic fault displacement hazard assessment (CRWMS M&O, 1998a). The repository layout with subareas, as defined in the NRC Total System Performance Assessment Code Version 4.1j, is shown in (b). Coordinates are in Universal Transverse Mercator (UTM) Zone 11, using the North American Datum of 1927.

Scientific Notebook 588E

Entry: John Stamatakos
Date: April 24, 2003

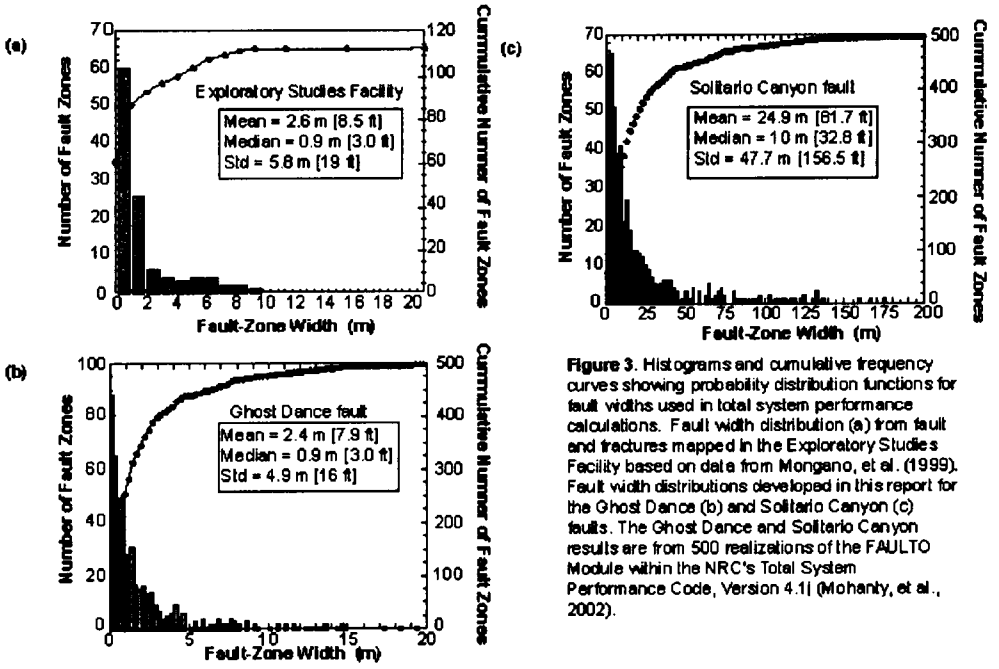

Figure 3. Histograms and cumulative frequency curves showing probability distribution functions for fault widths used in total system performance calculations. Fault width distribution (a) from fault and fractures mapped in the Exploratory Studies Facility based on data from Mongano, et al. (1999). Fault width distributions developed in this report for the Ghost Dance (b) and Solitario Canyon (c) faults. The Ghost Dance and Solitario Canyon results are from 500 realizations of the FAULTO Module within the NRC's Total System Performance Code, Version 4.1I (Mohanty, et al., 2002).

DATA:

IKONOS Satellite coverage is maintained in the **CNWRA GIS/Olympus database.**
Fault Coverage is maintained in the **CNWRA GIS/Olympus database.**

ESF Fault data extracted from DOE data in Mongano, et al., (1999) is in computer file ***ESF_Fault_Data.xls*,** which is attached as part of this electronic notebook. The data was transferred to **KaleidaGraph™ Version 3.09** to make the histograms. That data is in file ***ESF_Data.QDA*,** which is also attached as part of this electronic notebook.

From the resulting histogram (Figure 3a) we decided that the distribution was best fit as a lognormal distribution. We attempted some other curve fits (power and beta), but these other distributions could not replicate the observed ESF data as well as the lognormal distribution.

To model the distribution in the TPA code using the Latin Hypercube Sampler, we needed to supply the TPA code with the 0.999 and 0.001 probability values. To do this we used an **Excell(97-SR2)** Spreadsheet called ***LognormalDist.xls*** (which was developed for us by Consultant Robert Sewell and is now attached as part of this electronic record). In this spreadsheet we input the mean, median and/or standard deviation of the lognormal distribution we wanted to model. The spreadsheet then computes the probability distribution values including endpoints of the of the distribution. In this ***LognormalDist.xls*** spreadsheet we can get the $p = 0.9987$ and $p =$

0.00135 values. We used those to further extrapolate endpoints A and B, such that P(x<A) = 0.001 and P(x<B) = 0.999. We then tested this modleing and extrapolation by running the TPA code (500 realization) and plotted the resulting fault widths (figures 3b and 3c) to compare with the ESF data (Figure 3a). After several iterations we were able to get reasonable distributions in the TPA code that reasonably matched the observed distribution.

Because the Ghost Dance fault appears to be part of a continuum of secondary intra-block faults within the proposed Yucca Mountain repository footprint (figures 1 and 2), a probability distribution function was derived for fault-zone width of the Ghost Dance fault that matched the measured fault widths in the Exploratory Studies Facility (c.f., Figure 3a to Figure 3b). For the Solitario Canyon fault, a similar lognormal distribution shape was used (Figure 31c). Because the Solitario Canyon fault is a block-bounding fault, the mean value and standard deviation of the probability distribution function were adjusted to reflect substantially larger fault-zone widths, similar to fault-zone widths of the Solitario Canyon observed in the Cross Drift (Mongano, et al., 1999).

See: ***LognormalDist_Solitario_width.xls***
LognormalDist_GhostDance_width.xls

Table 1. Geometric Characteristics of the Solitario Canyon and Ghost Dance Faults

Parameter Description	Solitario Canyon Fault Distribution	Ghost Dance Fault Distribution
Center of the Fault (UTM, Zone 11, North American Datum 27).	Constant Northing = 4078000 Easting = 547600	Constant Northing = 4078200 Easting = 548400
Strike (degrees)	Constant 005°	Constant 005°
Trace Length (m) (Spans Length of Repository)	Constant 6000	Constant 6000
Width (m) 0.1 percentile 99.9 percentile	Lognormal $p_{0.001}$ = 0.294 $p_{0.999}$ = 339.5	Lognormal $p_{0.001}$ = 0.0116 $p_{0.999}$ = 62.8
NOTE: Information provided in meters; for conversion, use 0.31 m = 1 ft.		

b) Model WP failures

(1) set failure time to 100 yrs.

```
constant
TimeOfNextFaultingEventinRegionOfInterest[yr]
100.0
```

Subsequent runs were made for failure times of 2,000 yrs, 4,000 yrs and a uniform failure sample

between 100 and 10,000 yrs.

(2) set failure criteria (all WPs in fault zone fail - determined by fault width). This was done by setting the displacement to a constant of 1.0 m and the threshold displacement to constant of 0.5 m.

```
constant
ThresholdDisplacementforFaultDisruptionOfWP[m]
0.5

.....

constant
NWAmountOfLargestCredibleDisplacement[m]
1.0
```

(3) set release conditions (flow through/no drip shields)

```
** iflag
** FlowModelFlag(0=BathTub,1=FlowThrough)
** 1
```

(4) turn off drip shields by setting the drip shield failure time in the EBSFAIL module to 0 years and the drip shield thickness to 0.001 m [0.003 ft] in the NFENV module.

```
constant
DripShieldThickness[m]
0.001
.....

constant
DripShieldFailureTime[yr]
0.0
```

References:

Day, W.C., R.P. Dickerson, C.J. Potter, D.S. Sweetkind, C.A. San Juan, R.M. Drake, II, and C.J. Fridrich. "Geologic Map of the Yucca Mountain Area, Nye County, Nevada." U.S. Geological Survey Geologic Investigations Series, Map I–2627. Scale 1:24,000. 1998a.

Day, W.C., C.J. Potter, D.S. Sweetkind, R.P. Dickerson, and C.A. San Juan. "Bedrock Geologic Map of the Central Block Area, Yucca Mountain, Nye County, Nevada." U.S. Geological Survey Miscellaneous Investigations Series, Map I–2601. Scale 1:6,000. 1998b.

Mongano, G.S., W.L. Singleton, T.C. Moyer, S.C. Beason, G.L.W. Eatman, A.L. Algin, and R.C. Lung. "Geology of the Enhanced Characterization of the Repository Block Cross Drift—Exploratory Studies Facility, Yucca Mountain, Nevada." http://www.ymp.gov/timeline/site/ spg42gm3_a/. 1999.

Scientific Notebook 588E

Entry: John Stamatakos
Date: April 24, 2003

Entry 2. Annual Exceedence Probabilities from DOE PSHA Faulting Hazard

The probabilities of faulting were derived from the DOE fault displacement hazard curves (CRWMS M&O, 1998). We simply interpreted the displacements for the 20 cm and 1 m displacements, which were determined to be critical threshold values for waste package disruption. These values (20 cm and 1.0 m) were estimated based on recent DOE design for waste packages and drifts (CRWMS M&O, 2002) and assumptions of open or backfilled drifts.

CRWMS M&O. "Underground Layout Configuration: Subsurface Tunneling and Emplacement Drift Systems." 800–P0C–MGR0–00100–000–00A. Las Vegas, Nevada: CRWMS M&O. 2002.

———. "Probabilistic Seismic Hazard Analyses for Fault Displacement and Vibratory Ground Motion at Yucca Mountain, Nevada." WBS 1.2.3.2.8.3.6. Oakland, California: DOE. 1998.

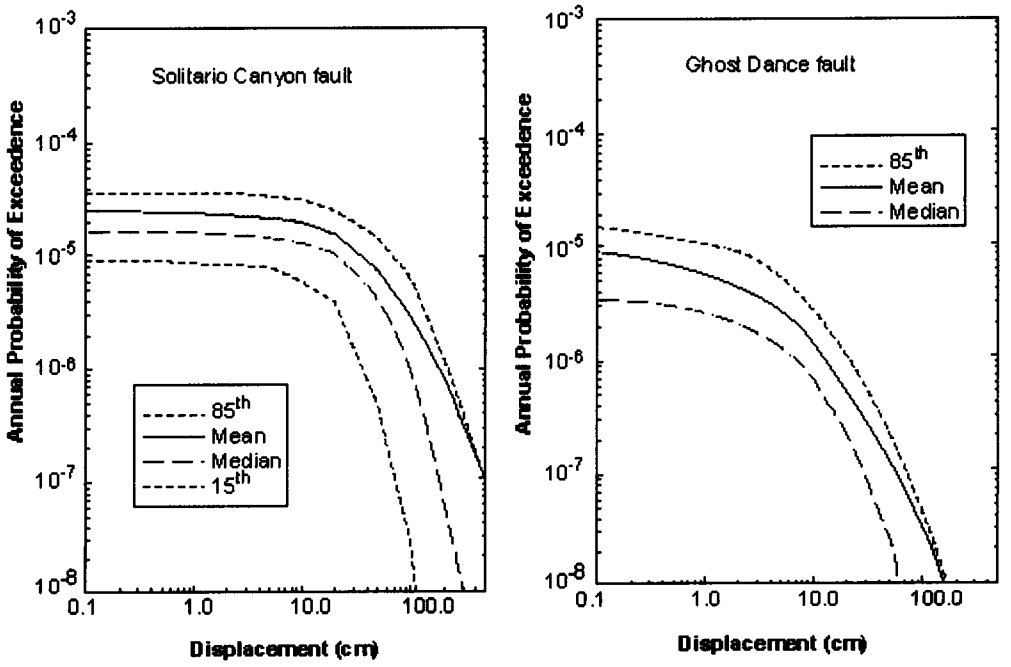

Figure 4. Probabilistic fault displacement hazard assessment curves for the Solitario Canyon and Ghost Dance faults. Images were scanned from CRWMS M&O (1998) and reformatted. To convert to English units, multiply displacements by 0.39 in/cm.

Entry: John Stamatakos
Date: April 24, 2003

Table 2. Annual Exceedence Probabilities for the Ghost Dance and Solitario Canyon Faults for 1 m [3.2 ft] and 0.2 m [0.64 ft] Fault Displacements			
		Annual Exceedence Probability	
Fault	**Statistical Measure**	**1.0 m [3.2 ft]**	**0.2 m [0.64 ft]**
Solitario Canyon	85th percentile	6×10^{-6}	2×10^{-5}
	Mean	3×10^{-6}	2×10^{-5}
	Median	9×10^{-7}	6×10^{-5}
	15th percentile	3×10^{-8}	4×10^{-6}
Ghost Dance	85th percentile	4×10^{-8}	6×10^{-7}
	Mean	3×10^{-8}	1×10^{-7}
	Median	$< 1 \times 10^{-8}$	3×10^{-7}
	15th percentile	$< 1 \times 10^{-8}$	$< 1 \times 10^{-8}$

Entry 3. TPA Conditional Dose Results

a) Set number of runs to 500 realizations

```
**
iconstant
NumberOfRealizations
500
**
```

b) We used the results in ***totdose.res***, which gave us the groundwater dose for each realization. These results were parsed using a simple script to create intermediate files that had a single column of time-steps and then 500 columns of data, one for each realization. This data was manipulated by **MATHEMATICA 4.1** functions to develop the statistical outputs. The driver file is ***comp.m.*** The sentences enclosed in "(* *)" are commented-out commands in **MATHEMATICA 4.1**, summarizing all that was done. Computations can be reproduced easily with the information in ***comp.m***. The files ***LeeDatos.m*** and ***quantilesM.m*** are the Mathematica packages that Osvaldo Pensado wrote to read the data and compute the statistics. The file ***comp.m*** uses the functions declared in ***LeeDatos.m*** and ***quantilesM.m.*** All these files are included as attachments to this electronic notebook.

c) The resulting data was then imported to **EXCELL (97-SR2)** spreadsheet for plotting and analysis. These data are stored in file ***Faulting_Milestone_042803_Total_Dose_Statistics.xls.*** Each TPA run is stored on a separate workbook page in the file.

d) Plotting was done using **KaleidaGraph™ Version 3.09**, because I find this software easier to use in making graphs. Figure 5 is an example plot showing the results for faulting at year 100.

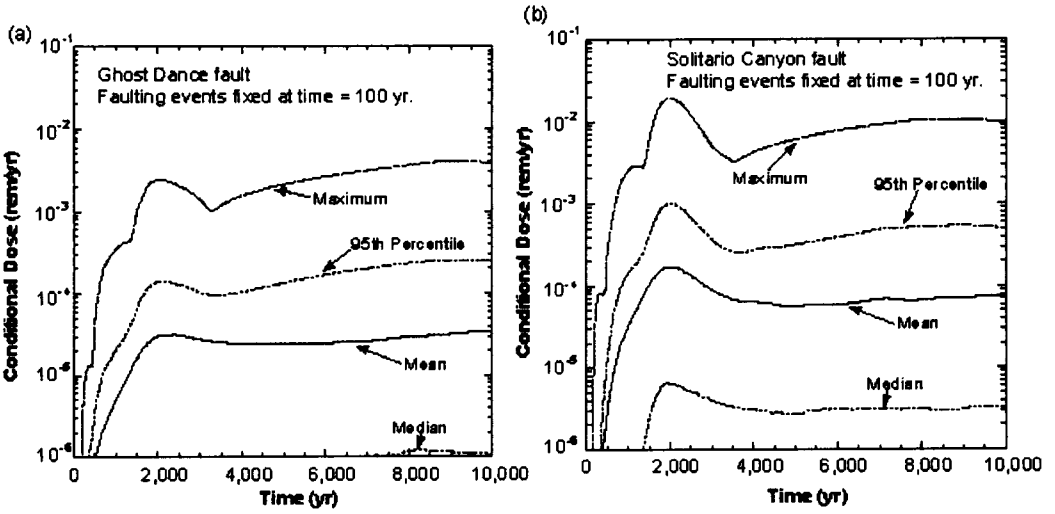

Figure 5 Graphical plots of the conditional doses through time in which faulting events are forced to occur at post-closure year100. Results are presented for the Ghost Dance (a) and Solitario Canyon (b) faults. The plots present the mean, median, 95th percentile, and maximum values of 500 realizations. In these calculations, all waste packages that fall within the zone of deformation around the named fault are assumed to fail and to permit release of radionuclides.

Entry 4: Risk Calculations

a) I used the dose-time results, in which faulting was forced to occur at year 2,000 and at year 4,000 or uniformly throughout the 10,000 years to show that the year-100 faulting gives the highest conditional doses (Figure 5).

b) To get to risk, we need to estimate the conditional doses that would occur from a faulting event in each year. To do this exactly is impractical because it would require 9,900 runs of 500 realization each - one for each year between year 100 and year 10,000. Instead, we interpolated a curve (red line in Figure 6) based on the 100-year faulting results which envelopes doses for faulting events in all later years. We then used this curve to estimate the conditional dose produced by faulting in each year. There are technical reasons why the 100-year faulting yields the largest conditional doses. The two most important of these are inventory decay of radionuclides and higher fuel solubility and dissolution during the thermal pulse early in the repository lifetime (see Mohanty, et al., 2002).

Mohanty, S., R. Codell, J.M. Menchaca, R.Janetzke, M. Smith, P. LaPlante, M. Rahimi, and A. Lozana. "System-Level Performance Assessment of the Proposed Repository at Yucca Mountain Using the TPA Version 4.1 Code." CNWRA 2002-05. Rev. 1.0. San Antonio, Texas: CNWRA. 2002.

c) The interpolated curve consists of 2 parts. There is a best-fit curve (fit to 100-year data) for the interval between year 100 and year ~ 2000 and a constant mean dose after that to year 10,000. The conditional mean dose (D_c) at time (t) between years 100 and 2000 is given by

$$D_c = A_0 + A_1 t + A_2 t^2 + A_3 t^3 + A_4 t^4$$

where t is time and A_0 to A_4 are coefficients given the following Table 3.

Table 3 Best-Fit Dose Versus Time Coefficients

Fault	Year of Maximum Conditional Mean Peak Dose	Maximum Conditional Mean Peak Dose (rem)	Best-Fit Polynomial Coefficients
Solitario Canyon	2,043	1.7×10^{-4}	$A_0 = -1.27 \times 10^{-6}$ $A_1 = 2.42 \times 10^{-8}$ $A_2 = -9.13 \times 10^{-11}$ $A_3 = 1.35 \times 10^{-14}$ $A_4 = -3.681 \times 10^{-17}$
Ghost Dance	2,251	3.2×10^{-5}	$A_0 = -1.9 \times 10^{-6}$ $A_1 = 1.58 \times 10^{-8}$ $A_2 = -3.63 \times 10^{-11}$ $A_3 = 3.61 \times 10^{-14}$ $A_4 = -8.94 \times 10^{-18}$

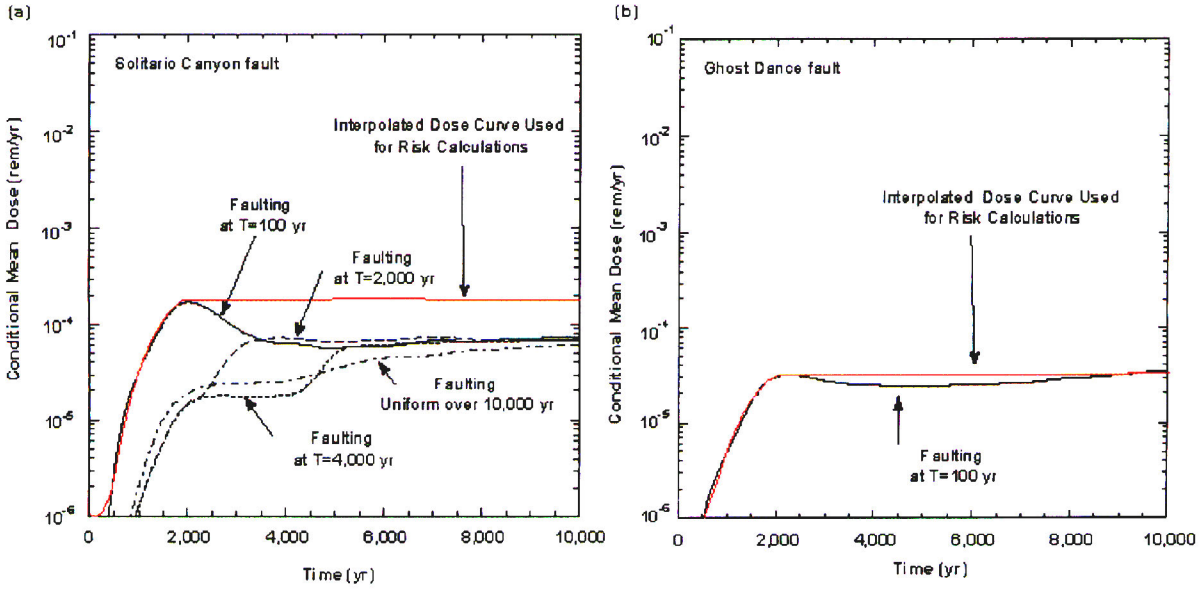

Figure 6. (a) Comparison of the mean dose-through-time curves for cases in which the faulting events on the Solitario Canyon fault were forced to occur in all 500 realizations at a specified year (100, 2,000, and 4,000) and for a case in which the faulting events occurred uniformly over the entire 10,000 yr post-closure period. The red line shows the interpreted dose-through-time curve used in the risk calculations. (b) Comparison of the conditional mean dose-through-time curve for faulting events on the Ghost Dance Fault that are forced to occur in all 500 realizations at year 100, compared to the interpolated time-dose curve used in risk calculations.

d) We used this formulation of the conditional mean dose to compute a conditional dose for each year between year 100 and year 10,000. This was done using **EXCELL (97-SR2)** and the data are stored in file ***Modeled_Dose_from_100_year_faulting.xls***.

e) The probability estimates used in the computation of risks were derived from the DOE probabilistic fault displacement hazard curves (Figure 4 and Table 2). Risk turn out to be small (Table 4) - also see the computation derived in ***Modeled_Dose_from_100_year_faulting.xls***.

Table 4. Risk Estimates for Faulting on the Solitario Canyon and Ghost Dance Faults

Fault	Mean Risk at Year 10,000 Assuming 0.20 m [0.67 ft] Threshold Fault Displacement (rem)	Mean Risk at Year 10,000 Assuming 1.0 m [3.2 ft] Threshold Fault Displacement (rem)
Solitario Canyon	3.1×10^{-5}	4.6×10^{-6}
Ghost Dance	2.7×10^{-8}	8.2×10^{-9}

Entry 5: Analog Fault Methodology - Fault trace length densities
(This entry was made by Dr. Alan Morris)

a) Maps of rupture traces digitized (Figure 7):
Rainbow Mountain-Stillwater
Borah Peak
Hebgen Lake
White Mountains Front (Chalfant Valley)

This data is contained in the Excel files:
Rainbow_sm_sourcedata.xls
Borah_flts_sourcedata.xls
Hebgen_flts_sourcedata.xls
WhiteMtn_FZ_sourcedata.xls

These Excel files also contains the segment lengths and overall fault density data for these data sets.

b) Using a 100 m x 100 m moving window (each move increment is 50 m in both the X and Y directions), the fault density (km of rupture length per square km) was measured over the entire area. The file ***FaultDensity.rtf*** contains the algorithms used for this analysis.

c) Output from this analysis is contained in the files
AllFaultDensity_April2003.xls
AllFaultDensity_cumulativeplot.xls

Scientific Notebook 588E

Entry: John Stamatakos
Date: April 24, 2003

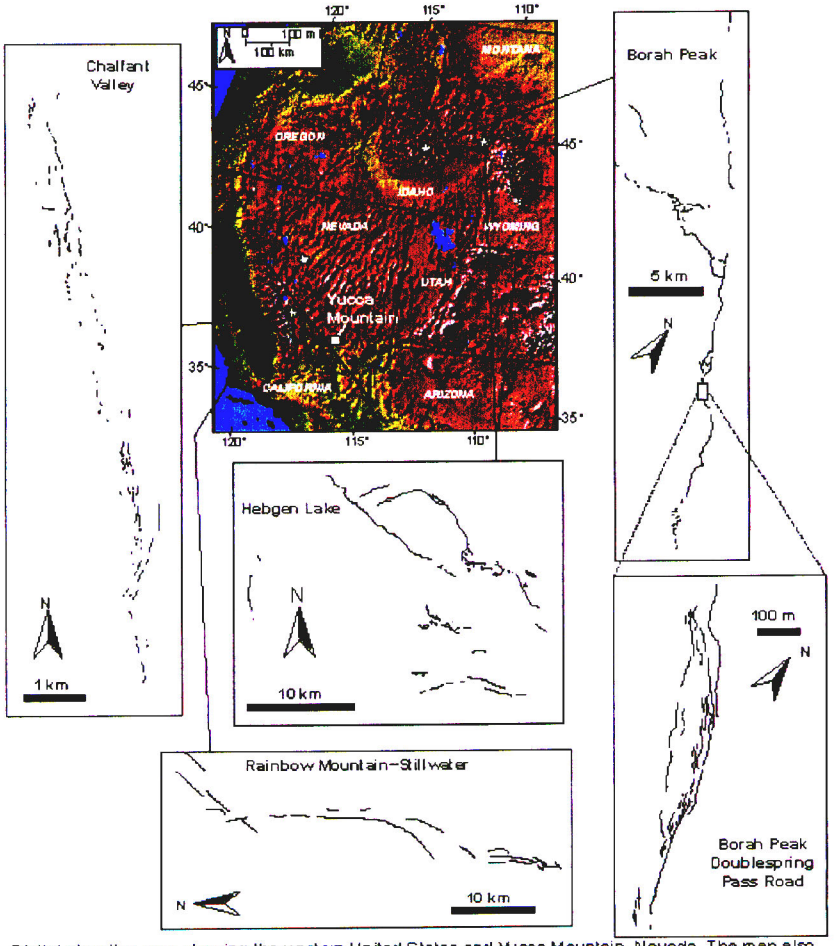

Figure 7. Digital elevation map showing the western United States and Yucca Mountain, Nevada. The map also shows the location of four earthquakes in the western United States that produced ground rupture. Insets show maps of rupture traces for each of the four analog events, Chalfant, Borah Peak, Rainbow Mountain—Stillwater, and Hebgen Lake. Also shown is an inset of a detailed portion of the Borah Peak fault ruptures near Doublespring Pass Road, adapted from Crone, et al., (1987).

d) A portion of the map: Day, W. C., C. J. Potter, D. S. Sweetkind, R. P. Dickerson, and C. A. San Juan. Bedrock Geologic Map of the Central Block Area, Yucca Mountain, Nye County, Nevada, U.S. Geol. Surv. Misc. Invest. Ser. Map, I-2601, 1998 was abstracted (***day_flys_trimmed2.xls***) and treated as in (b) above. The results of this analysis are in ***day_flts_trimmed_map.xls.***

e) The abstracted data from the Day et al., 1998 map were analyzed for fault density using a 1000 m x 1000 m moving window (each move increment is 500 m in both X and Y directions). The results of this are in ***DAY_sampledat1k.xls.***

f) Based on these analyses we selected a value of 5 km/km^2 as representative of the fault trace-length densities at Yucca Mountain. This values is near average for the four fault analogs and is the average for fault at Yucca Mountain.

Entry 6: Drift Intersection Analysis

Scientific Notebook 588E

Entry: John Stamatakos
Date: April 24, 2003

(This entry was derived from input supplied to John Stamatakos by Dr. Alan Morris)

The number of drifts possibly intersected by faulting depends on several geometric characteristics of the faults and engineered drifts. The number of potential fault-drift intersections depends on the spatial density of faults, spacing of the drifts, and azimuth of the drifts relative to the fault traces. To quantify the number of drift intersections for a given faulting event, a geometric model was constructed (Figure 8). The fault population is modeled as straight, parallel, equally spaced lines inscribed within a circle so that one line represents a diameter (population A, Figure 8a). Engineered drifts are modeled as a second population of straight, parallel, equally spaced lines drawn within the circle so that no line passed through the center of the circle (population B, Figure 8a).

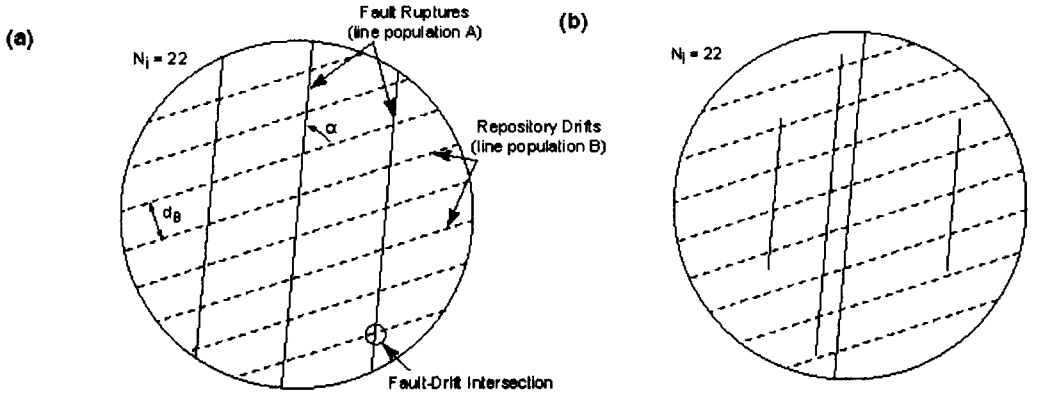

Figure 8. Diagram illustrating the parameters used in Eq. 4-1, in which the number of drift-fault intersections is estimated based on the number and orientation of faults and the orientation and spacing of repository drifts. In both examples shown in (a) and (b), the number of fault-drift intersections (N_i) is equal to 22.

The number of intersections between the two populations of lines within the circle depends on the spacing of the two populations and the angle between them and can be approximated by the relationship:

$$Ni \approx \left[\frac{\sin(\alpha)}{d_B}\right] \times \Sigma L_A \qquad (1)$$

Where Ni is the number of intersections within the circle, is the angle between two line populations, LA is the total line length of fault traces within the circle (population A), and dB is the spacing of drifts within the circle (population B). Because Ni represents the number of fault-drift intersections, it is an integer value.

Equation 1 is written as the line length of one population within the sampled area and the spacing of the other population. This formulation is convenient because the spatial density of distributed fault arrays, which are anastomosing and irregular, is best characterized by the trace length per unit area (as described in the preceding section); whereas, the regular pattern of the drifts is easily represented by drift spacing. Ni can be expressed as the number of drift-fault trace intersections per unit area (divided by the area of the circle). This number can then be used to estimate the total number of intersections for any given area.

The geometric model for evaluating fault-drift intersections is versatile and robust. Shifting the line populations so

they are not symmetrically disposed within the circle has little effect on the resulting number of intersections (±1) except in the limiting cases where one or more of the lines in one population is coincident with a line or lines in the other population. In addition, maintaining the total length of population A, but permitting it inconsistent spacing and distribution (i.e., lines terminating within the circle and not at the perimeter), has little effect on the number of drift-fault intersections (±1) (Figure 8b).

Entry 7: Fault-Drift Intersections.

a) Repository Design (CRWMS M&O, 2002) indicates a drift azimuth of 072° and a drift spacing of 81 m [265.7 ft].

b) The mean azimuth of faults at Yucca Mountain is 005° (see rose diagram in Figure1). Thus, the angle α between dominant fault trace and the drift orientation is equal to 67°.

c) From these values, the estimated number of fault-drift intersections likely to result from an earthquake event at Yucca Mountain as a function of fault density and repository area was calculated (Figure 9) - see Excell file - ***Drift-Fault_Intersections.xls***. Total repository area for this recent design depends on the number of panels ultimately used. Current DOE plans indicate that not all the panels shown in this design will be used, and, thus, the repository will encompass an area between 5 km^2 and 7 km^2 [1.9 mi^2 and 2.7 mi^2].

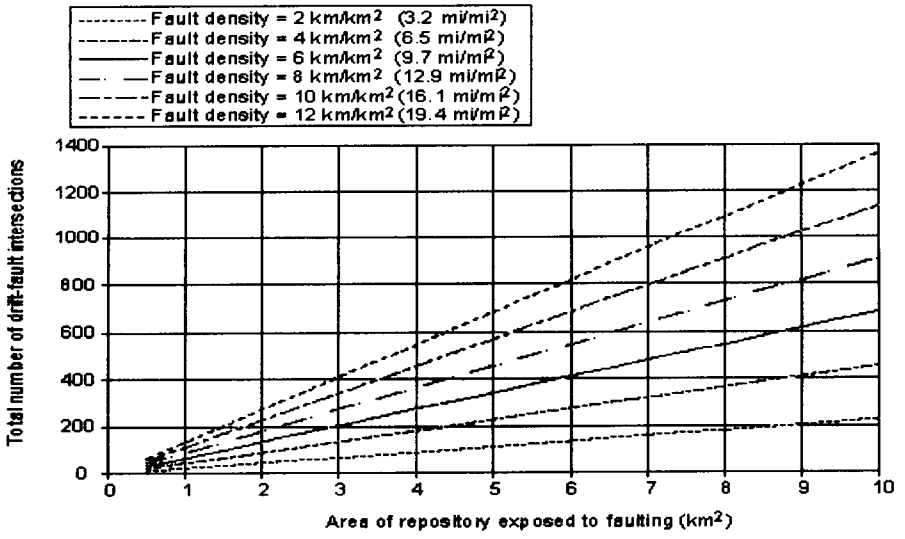

Figure 9. Graph of the total number of drift-fault intersections for a series of fault density values as a function of repository area.

e) Assuming a distributed fault density of 5 km/km^2 [8 mi/mi^2] that was estimated from the fault density data described in the Enrty 5, the graph in Figure 9 indicates 143 and 200 fault-drift intersections. If it is assumed that all fault-drift intersections lead to waste package failures, this analysis estimates 143–200 conditional waste package failures could occur from a large faulting event.

Scientific Notebook 588E

Entry: John Stamatakos
Date: April 24, 2003

Entry 8: Conditional Dose

a) The 143-200 waste package failures were forced to occur in all TPA Version 4.1j code realizations at postclosure year 100. This was accomplished by using the defective fraction of WPs/cell parameter in the TPA code. The fraction is obtained by dividing the number of intersected WPs by 8877 (total number of WPs in the repository.

200/8877 = 0.02255301
143/8877 = 0.016109

```
**
constant
DefectiveFractionOfWPs/cell
0.0225
```

b) Except for the use of the juvenile failure parameter, other conditions of the TPA Version 4.1j code were the same as those used in the FAULTO module methodology. The TPA Version 4.1j code run consisted of 500 realizations of the code to ensure statistically reliable results. The beneficial effects of the drip shield were removed as before. The full range of parameters in the standard base case input file was sampled in each realization.

c) Results of conditional dose versus time for faulting events are shown in Figure 10. Similar to those curves shown in Figure 6, the dose versus time curves show an initial peak within approximately 2,000 years of the faulting event, indicating an influence of the thermal pulse on initial solubility rates of radionuclides. The curves also show a steady increase in dose, reaching a second maximum at year 10,000. The maximum mean peak conditional dose in this example calculation is 2.9×10^{-5} rem, which occurs at approximately year 3,000.

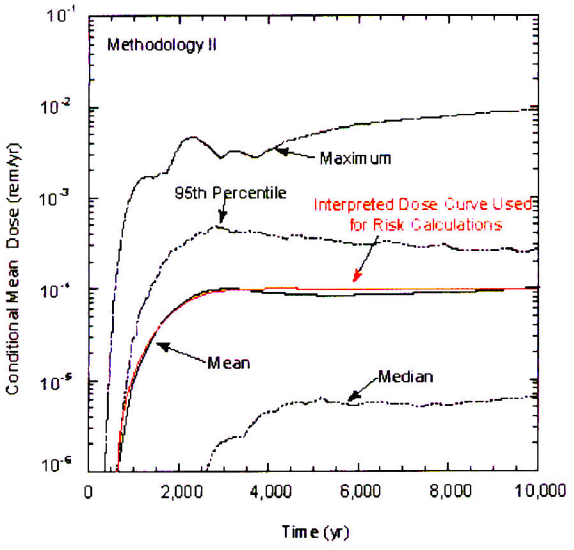

Figure 10. Graphical plots of the conditional doses through time for Methodolgy II. Faulting is abstracted as juvenile failures, forced to occur at year 100. Results are presented for the mean, median, 95th percentile, and maximum values of 500 realizations. The red curve is the interpreted dose-through-time curve used in the risk calculations.

d) Results are in ***Faulting_Milestone_042803_Total_Dose_Statistics.xls.*** These statistical results were obtained in the same way as those in Entry 3.

Entry 9: Risk

a) Risk was computed in the same was as described in Entry 4. The interpolated function for the red line shown in figure 10 has a form:

$$D_c = A_0 + A_1 t + A_2 t^2 + A_3 t^3$$

Table 5. Best-Fit Dose Versus Time Coefficients		
Year of Maximum Conditional Mean Peak Dose	**Maximum Conditional Mean Peak Dose (rem)**	**Best-Fit Polynomial Coefficients**
3,163	2.9×10^{-5}	$A_0 = 1.58 \times 10^{-6}$ $A_1 = -1.96 \times 10^{-8}$ $A_2 = 2.75 \times 10^{-11}$ $A_3 = 1.37 \times 10^{-14}$

b) Thus the interpolate values were calculated for years 100 to 3,200. A constant value of 2.9×10^{-5} was used for years 3,200-10,000. See Excell file ***Modeled_Dose_method_II_risk.xls.***

c) Probability weights were derived from the DOE PSHA results. For example, maximum fault displacement for the Borah Peak earthquake, as measured by Crone, et al. (1987), was 2.7 m [8.9 ft], with an average displacement of approximately 1 m [3.2 ft]. The mean annual exceedence probabilities for 1 m [2.6 ft] of displacement for faults at Yucca Mountain (CRWMS M&O, 1998) range between 5×10^{-6}/yr for the Solitario Canyon fault to 3×10^{-8}/yr for the Ghost Dance fault.

d) Risk estimates, based on these probabilities, range between 4.0×10^{-6} and 2.4×10^{-8} rem/yr. This risk computation is also in the attached Excell spreadsheet - ***Modeled_dose_method_II_risk.xls***.

I have reviewed scientific notebook E 588 and find it in compliance with QAP-001. There is sufficient information regarding procedure used for conducting the research and acquiring and analyzing the data so that another qualified scientist could repeat the activity or activities recorded in this scientific notebook. This notebook and accompaning files are to be archived and the notebook closed.

H. Lawrence McKague
GLGP Element Manager
Reviewed 05/07/03

ADDITIONAL INFORMATION FOR SCIENTIFIC NOTEBOOK No.: 588E

Document Date:	04/24/2003
Availability:	Southwest Research Institute® Center for Nuclear Waste Regulatory Analyses 6220 Culebra Road San Antonio, Texas 78228
Contact:	Southwest Research Institute® Center for Nuclear Waste Regulatory Analyses 6220 Culebra Road San Antonio, TX 78228-5166 Attn.: Director of Administration 210.522.5054
Data Sensitivity:	■"Non-Sensitive" □ Sensitive □"Non-Sensitive - Copyright" ☐ Sensitive - Copyright
Date Generated:	04\24\2003
Operating System: (including version number)	Windows 2000
Application Used: (including version number)	WordPerfect 10; Adobe Illustrator 8.0; Acrobat 5.0; Microsoft Excel 2000; PowerPoint 2000; Word 2000
Media Type: (CDs, 3 1/2, 5 1/4 disks, etc.)	1 CD
File Types: (.exe, .bat, .zip, etc.)	wpd, ai, pdf, xls, ppt, doc, inp, m, p, qda
Remarks: (computer runs, etc.)	Media contains: Data files for evaluation of faulting related to postclosure performance of the proposed Yucca Mountain repository.